引用格式：CUI Fengxiang, BAI Yanli, WU Siqi, et al. Research on the Picoseconds Gating Pulse of Framing Camera Using Pulse Steepening Technique[J]. Acta Photonica Sinica, 2023, 52(1):0125001
崔逢祥,白雁力,伍思其,等.基于脉冲陡化技术的皮秒分幅相机选通脉冲研究[J].光子学报,2023,52(1):0125001

基于脉冲陡化技术的皮秒分幅相机选通脉冲研究

崔逢祥,白雁力,伍思其,陈欢,梁禄业,朱云斐,谢军
(桂林电子科技大学 电子工程与自动化学院,桂林 541004)

摘　要:为获得高幅值和窄半高宽的选通脉冲,基于雪崩三极管Marx脉冲发生器和脉冲陡化技术,设计皮秒高压脉冲电路,对应用于分幅相机的选通脉冲展开研究,并采用蒙特卡洛法建立微通道板通道内的光电子动态倍增研究模型,通过将选通脉冲应用于微通道板增益计算获取时间分辨率。研究结果表明,基于Marx脉冲发生器和脉冲陡化技术相结合产生皮秒选通脉冲的方法是可行的,当Marx脉冲发生器为三级,脉冲陡化电路的两个电感和电容分别为725 nH、7 nH、1 pF时,可获得幅值−2.8 kV和半高宽124 ps的选通脉冲。将该选通脉冲加载于微通道板上进行光电子动态倍增过程研究,通过分析和统计微通道板增益,获得分幅相机的时间分辨率约为53 ps。

关键词:分幅相机;脉冲陡化技术;选通脉冲;蒙特卡洛法;时间分辨率
中图分类号:TB872;TM836　　**文献标识码**:A　　**doi**:10.3788/gzxb20235201.0125001

0　引言

惯性约束聚变(Inertial Confinement Fusion,ICF)是获取热核武器实验数据的主要途径[1-2],由于微通道板(Microchannel Plate,MCP)分幅相机具有皮秒级时间分辨和微米级空间分辨,因此在ICF实验中能有效探测聚变过程的等离子体时空演化状态[3]。MCP分幅相机的时间分辨率约为60～100 ps[4],主要影响因素是MCP通道内的电子渡越时间及其渡越时间弥散,改善方法主要包括薄MCP和优化选通脉冲两种,薄MCP虽然能有效提升相机时间分辨率,但由于薄MCP信噪比差且制作工艺要求高[5],因此难以广泛应用,所以提高MCP分幅相机时间分辨率,常通过优化电路结构,以获得高幅值和窄半高宽的皮秒选通脉冲来实现[6]。

皮秒高压脉冲是脉冲功率技术的一个分支,通常先对低功率能量进行储存,然后在极短时间内释放能量,以此输出高功率脉冲[7],而应用于MCP分幅相机的皮秒选通脉冲可通过纳秒高压脉冲和脉冲成形实现。在纳秒高压脉冲方面,由于雪崩三极管在雪崩状态下具有快速导通的开关特性,因而在脉冲发生器中获得广泛应用[8-9],但在不同电路结构下,会出现高压放电打火和容易被击穿损坏的情况[10]。在脉冲成形方面[11-13],通常采用专门的形成线路技术和脉冲陡化技术实现皮秒脉冲的输出,前者是通过对脉冲能量压缩实现脉冲时间宽度和功率的大幅度减小,后者是通过对脉冲前后沿陡化实现脉冲时间宽度的压缩,对脉冲功率影响相对较小。

为改进传统雪崩三极管电路稳定性的不足,获得皮秒高压的分幅相机选通脉冲,采用雪崩三极管串并联的混合方式设计Marx脉冲发生器和基于脉冲陡化技术设计脉冲成形电路,并将输出的选通脉冲应用于MCP分幅相机时间分辨率计算。首先基于雪崩三极管设计Marx脉冲发生器,并分析电路参数对输出纳秒

基金项目:国家自然科学基金(No. 11865007),广西省自然科学基金 (No. 2022GXNSFAA035561),广西自动检测技术与仪器重点实验室主任基金(No. YQ22101)
第一作者:崔逢祥,cfx17863525480@163.com
通讯作者:白雁力,bayaly@guet.edu.cn
收稿日期:2022-06-06;**录用日期**:2022-08-22

脉冲影响；然后基于脉冲陡化技术设计脉冲成形电路，分析电路参数对皮秒选通脉冲的影响；最后，采用蒙特卡洛法建立MCP通道内的光电子动态倍增研究模型，将选通脉冲应用于MCP增益计算获取时间分辨率。

1 基于雪崩三级管的Marx脉冲发生器设计

Marx发生器是脉冲功率技术中用来获得高幅值和纳秒半高宽脉冲的一种常用装置[7]。采用雪崩三极管串并联的混合方式设计的N级Marx脉冲发生器如图1，第一级由雪崩三级管Q_{11}～Q_{18}、直流电源V_1、方波触发信号源V_{21}、微分电路（电容C_{21}和电阻R_{21}组成）、主电容C_{11}和限流电阻R_{11}～R_{12}构成。由于单个雪崩三极管作为开关时导通电压较小，为提高单级电路导通电压，采用Q_{11}～Q_{18}串联整体作为开关，而单级雪崩三极管串联个数取决于三极管型号和每级目标输出幅值；C_{21}和R_{21}组成微分电路，具有把方波触发信号转换为上升沿陡峭触发信号的功能。系统工作流程为：当未加载触发信号时，雪崩三极管处于截止状态，各级电路为并联状态，V_1通过限流电阻给主电容充电；当加载触发信号时，第一级雪崩三极管Q_{11}触发导通，Q_{12}～Q_{18}过压击穿导通，同理第2级到第N级雪崩三极管也依次导通，各级主电容串联放电，最后在负载R上输出纳秒高压脉冲。N级Marx脉冲发生器输出脉冲的幅值V_{MARX}可表示为

$$V_{MARX}=\frac{-V_1}{1-N\times D} \tag{1}$$

式中，N为电路级数，V_1为输入直流电压，D为方波触发信号源V_{21}的占空比。

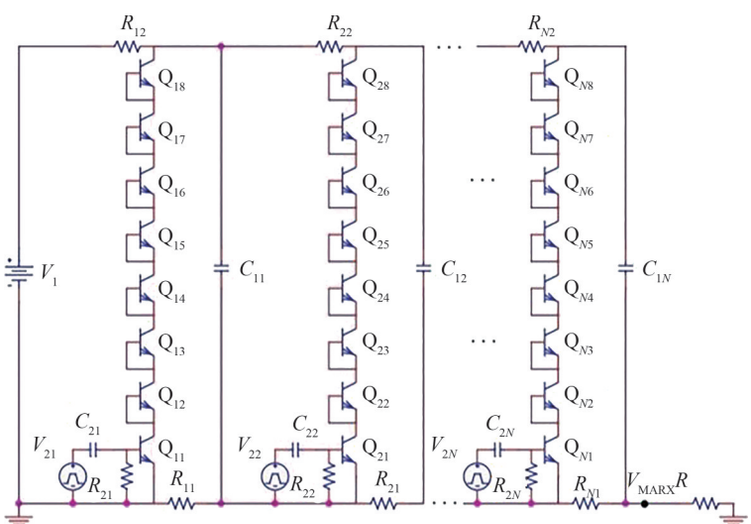

图1 基于雪崩三极管的N级Marx脉冲发生器设计

Fig.1 Design of N-stage Marx pulse generator based on avalanche triode

设计时，雪崩三极管采用2N5551，其雪崩击穿电压约为480 V。为实现脉冲发生器高幅值输出，同时降低电路复杂度，要求每一级发生电路尽可能地串联多个雪崩三极管以提高输出幅值，但受限于雪崩三极管串联个数过多会导致高压打火等降低发生器稳定性的情况，因此各级雪崩三极管个数不宜过多，综合考虑在设计中采用8个雪崩三级管串联构成一级发生电路。当直流电源V_1为3.7 kV，限流电阻R_{11}～R_{N2}为150 kΩ，主电容C_{11}～C_{1N}为2 nF的高压陶瓷电容，负载电阻R_{10}为200 Ω，微分电路电容C_{21}～C_{2N}为10 μF和电阻R_{21}～R_{2N}为100 Ω时，基于雪崩三极管的Marx脉冲发生器随着级数N变化的输出脉冲波形如图2。随着发生器级数N从1增加到5，脉冲半高宽从165.298 ns增大到165.924 ns，幅值从－2.019 kV增大到－10.098 kV，同时由于回路分布电感逐渐增大导致脉冲幅值增量逐渐减小[8]。当发生器级数N为3时，输出幅值约为－6 kV已达到输出目标，考虑到发生器的输出幅值效率应尽可能大，脉冲半高宽应尽可能小，采用基于雪崩三极管的三级Marx脉冲发生器设计实现纳秒高压脉冲，对应输出脉冲V_{MARX}幅值为－6.058 kV，半高宽为165.924 ns，前沿时间为68.231 ns，后沿时间为129.407 ns，脉冲功率为182.892 kW。

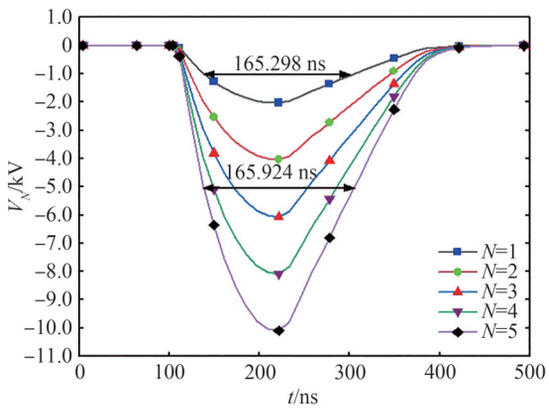

图2　不同电路级数下纳秒脉冲幅值曲线

Fig.2　Output pulse amplitude curves with different stages

2　基于脉冲陡化技术的脉冲成形电路设计

基于雪崩三极管的Marx脉冲发生器输出脉冲只能达到纳秒，要实现皮秒高压脉冲，可在保证脉冲输出幅值的基础上，基于脉冲陡化技术设计脉冲成形电路，通过对脉冲前后沿陡化实现脉冲时间宽度的压缩。脉冲陡化原理是通过纳秒级脉冲对小容量电容进行快速充放电的方法，在损耗部分脉冲幅值的同时缩短脉冲前沿时间，通过降低脉冲后沿的拖尾方法，缩短脉冲后沿时间，经过陡化后输出的脉冲达到皮秒。基于脉冲陡化技术的脉冲成形电路如图3，主要由电感L_1和L_2、电容C_7、负载电阻R_{10}以及自击穿陡化开关U_1和U_2组成。系统工作时，首先，基于雪崩三极管的Marx脉冲发生器输出的纳秒级高压脉冲V_{MARX}经过L_1对C_7快速充电；然后，当C_7上电压达到峰值时，U_1自击穿导通，C_7快速放电，产生具有极快下降前沿的脉冲V_{QD}；接着，V_{QD}经过L_2对R_{10}放电；最后，当R_{10}上电压达到峰值时，U_2自击穿导通，产生具有极快上升后沿的脉冲V_{HD}，纳秒级脉冲经过脉冲成形电路后达到皮秒。

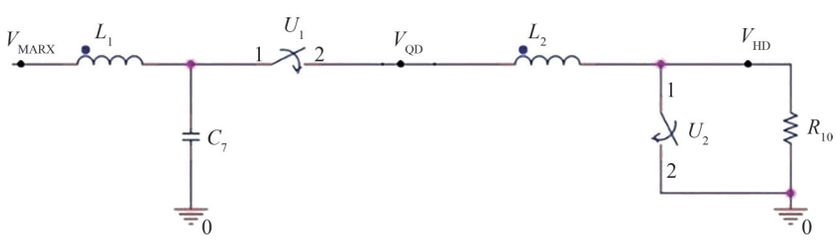

图3　基于脉冲陡化技术的脉冲成形电路

Fig.3　Pulse shaping circuit based on pulse steepening technique

在脉冲成形电路中保持输入的纳秒脉冲为V_{MARX}不变，不同电感L_1（500～900 nH）和L_2（5～9 nH），电容C_7（1～5 pF）和负载电阻R_{10}（50～250 Ω）对脉冲成形电路输出皮秒选通脉冲的影响如图4。图4（a）为L_1对皮秒选通脉冲的影响，当L_2为7 nH，C_7为1 pF和R_{10}为200 Ω时，随着L_1从500 nH到900 nH，脉冲幅值和半高宽变化相对较小，所以通常在保证脉冲输出的基础上，可采用较小的电感设计。图4（b）为L_2对皮秒选通脉冲的影响，当L_1为725 nH，C_7为1 pF和R_{10}为200 Ω时，随着L_2从5 nH到9 nH，脉冲前沿时间从38 ps增长到51 ps，幅值从－2.999 kV减小到－2.761 kV，所以采用较小的L_2有助于脉冲前沿时间的缩短。图4（c）为C_7对皮秒选通脉冲的影响，当L_1为725 nH，L_2为7 nH和R_{10}为200 Ω时，随着C_7从1 pF到5 pF，脉冲前沿时间从47 ps缩短到31 ps，后沿从31 ps增长到37 ps，幅值从－2.867 kV减小到－1.184 kV，所以适当减小C_7是缩短脉冲前后沿时间和增大脉冲幅值的有效方法。图4（d）为R_{10}对皮秒选通脉冲的影响，当L_1为725 nH，L_2为7 nH和C_7为1 pF时，随着R_{10}从50 Ω到250 Ω，脉冲前沿时间从71 ps缩短到15 ps，后沿从15 ps增长到36 ps，幅值从－1.472 kV增大到－3.048 kV，所以负载过小会导致较小的脉冲幅值和较大的脉冲前沿，负载过大会导致较大的脉冲后沿，而且随着负载的增大负载增量会逐渐变少，考虑到电路输出要作为选通脉冲应用于MCP分幅相机时间分辨率计算，因此保证脉冲幅值和前后沿时间宽度的基础上，尽可能地使脉冲输出前后沿

近似对称。在基于脉冲陡化技术的脉冲成形电路设计中取L_1为725 nH，L_2为7 nH，C_7为1 pF和R_{10}为200 Ω，输出的皮秒高压选通脉冲V_{HD}如图5，其脉冲幅值为−2.87 kV，前沿时间为47 ps，后沿时间为31 ps，半高宽为124 ps，脉冲功率为40.898 kW。

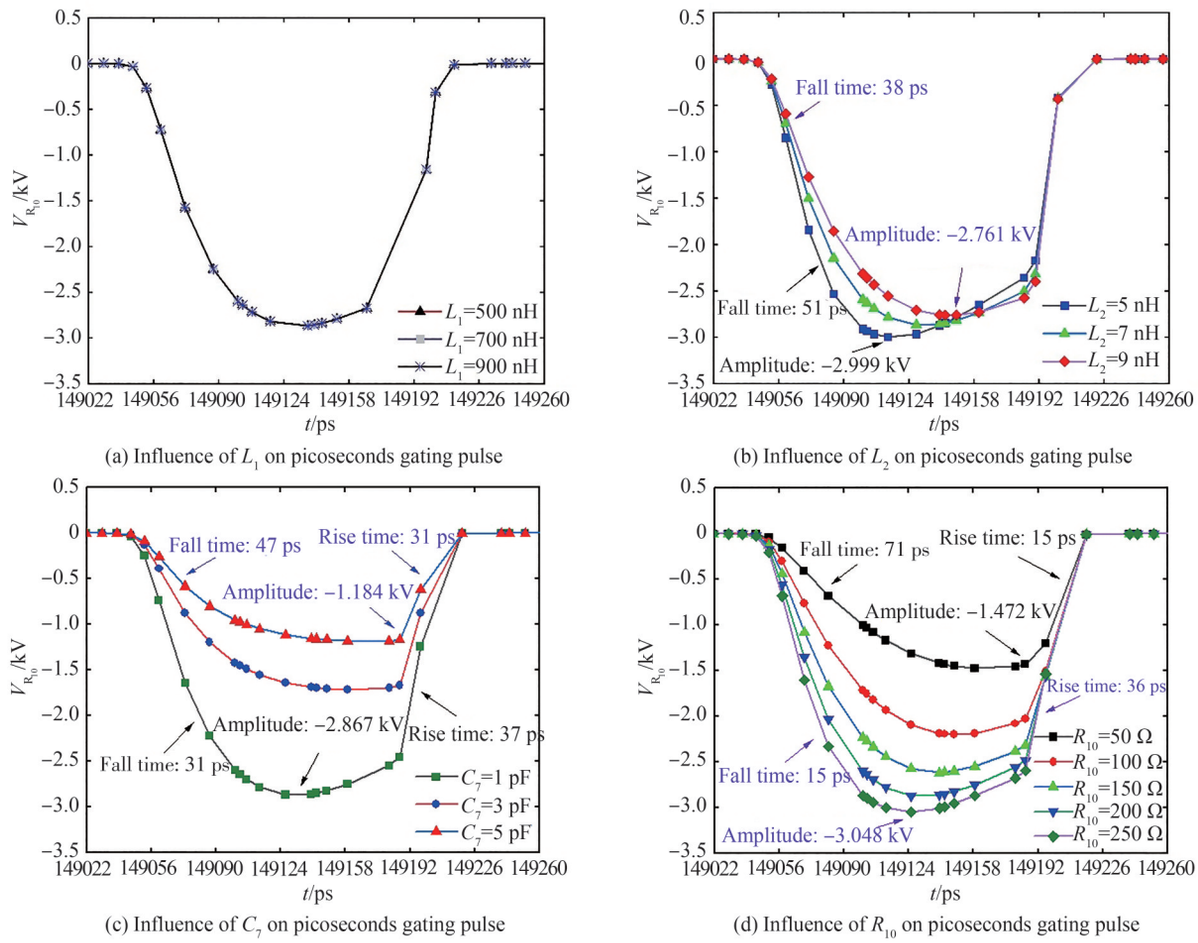

(a) Influence of L_1 on picoseconds gating pulse

(b) Influence of L_2 on picoseconds gating pulse

(c) Influence of C_7 on picoseconds gating pulse

(d) Influence of R_{10} on picoseconds gating pulse

图4 电路参数对皮秒选通脉冲的影响

Fig.4 Influence on picoseconds gating pulse with different circuit parameters

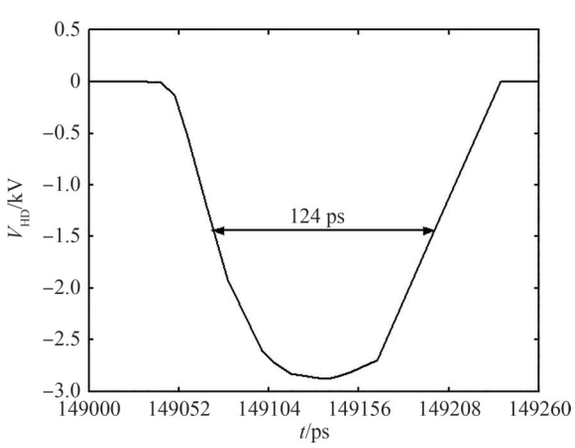

图5 皮秒高压选通脉冲

Fig.5 High voltage gating pulse with picoseconds

3 MCP分幅相机时间分辨率计算

MCP分幅相机的时间分辨率是指MCP的增益-时间曲线半高宽，为计算时间分辨率，需要将选通脉冲

加载于MCP上，通过研究MCP通道内光电子动态倍增过程和计算MCP增益，最后建立MCP的增益-时间曲线。具体分析过程为：首先，将选通脉冲加载于MCP上，并对光电子发射参数初始化；然后，建立MCP通道内光电子动态倍增过程研究模型，计算光电子在MCP通道内，经过碰撞通道壁后产生的二次电子数目、轴向位移和传输时间，并根据二次电子能量和发射角模型计算下一次碰撞后的二次电子出射参数，直到光电子传输出MCP的通道；最后，统计选通脉冲不同时刻的MCP增益，建立增益-时间曲线，获取MCP分幅相机的时间分辨率。

MCP分幅变像管结构如图6，其中L为MCP通道长度，d为MCP通道直径，θ为MCP斜切角，L_1为MCP与荧光屏（phosphor screen）之间的距离。由于MCP斜切角的存在，因此分幅变像管是非轴对称的，为便于计算，在MCP通道内建立$w'v'u'$坐标系，在MCP与荧光屏间建立wvu坐标系。

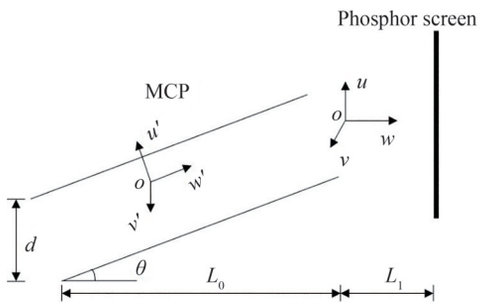

图6　MCP分幅变像管结构

Fig.6　Structure of MCP framing image converter

基于蒙特卡洛法模拟MCP内光电子动态倍增过程中的增益计算方法[14]如式(2)～(10)。式(2)和式(3)分别为光电子发射能量和发射角分布；光电子在通道内的碰撞时刻如式(4)，其中t_i和t_{i-1}分别为第i和$i-1$次的碰壁时刻，d是MCP通道直径，$E_{or(i)}$为第i次发射能量的径向分量；式(5)为第i次碰撞的轴向位移Z_i，其中$E_{oz(i-1)}$是第$i-1$次发射能量的轴向分量，V_{HD}为皮秒级高压选通脉冲，L是MCP厚度，e和m分别是电子的电荷量和质量；式(6)为光电子第i次碰撞总能量E_i，其中第i次碰撞总能量的径向分量$E_r(i)$和轴向分量$E_z(i)$分别如式(7)和式(8)；式(9)为第$i+1$次光电子发射能量$E_{o(i+1)}$，其中β是能量损耗比例常量，与所选MCP材料和制作工艺有关；式(10)为所有抽样光电子产生的增益G，其中n为抽样光电子个数，E_c是二次电子发射系数为1时的碰撞能量，k为与MCP材料和制作工艺有关的常数[14-15]。

加载于MCP上的选通脉冲如图5，其幅值为－2.8 kV，半高宽为124 ps。当MCP的参数d=12 μm、L=0.5 mm、θ=6°、β=2.47、E_c=29.4 eV，k=0.75和MCP直流偏置电压为－300 V时，采用蒙特卡洛法，通过式(2)～(10)计算获得MCP的归一化增益曲线如图7，其半高宽为53 ps，即MCP分幅相机的时间分辨率。

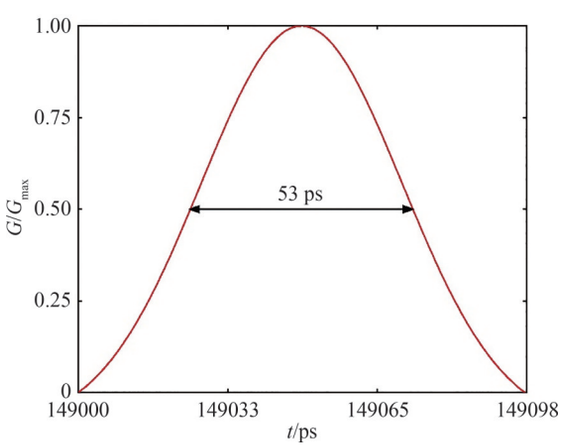

图7　MCP增益-时间曲线归一化

Fig.7　Curve of MCP normalized gain

$$f(E)=\frac{250\times E}{(E+3.7)^4} \tag{2}$$

$$f(r)=\begin{cases}\dfrac{1}{2} & r\in[-1,+1]\\ 0 & r\in(-\infty,-1)\cup(+1,+\infty)\end{cases} \tag{3}$$

$$t_i=t_{i-1}+d/\sqrt{2E_{or(i)}/m} \tag{4}$$

$$E_i=\int_{t_i-1}^{t_i}\sqrt{\frac{2E_{oz(i-1)}}{m}}\,\mathrm{d}t+\int_{t_i-1}^{t_i}\frac{e\int_{t_{i-1}}^{t_i}V_{\mathrm{HD}}\,\mathrm{d}t}{mL}t\mathrm{d}t \tag{5}$$

$$E_i=\sqrt{E_{or(i-1)}^2+E_{z(i)}^2} \tag{6}$$

$$E_{r(i)}=E_{or(i-1)} \tag{7}$$

$$E_{z(i)}=\frac{1}{2}\times m\times\sqrt{\frac{2E_{oz(i-1)}}{m}}+\frac{2}{500}\times\int_{t_{i-1}}^{t_i}\frac{e\int_{t_{i-1}}^{t_i}V_{\mathrm{HD}}\,\mathrm{d}t}{mL}\mathrm{d}t \tag{8}$$

$$E_{o(i+1)}=E_i/4\beta^2 \tag{9}$$

$$G=\frac{1}{n}\sum_{j=1}^{n}\left(\prod_{i=1}^{j}(E_i/E_c)^k\right) \tag{10}$$

4 结论

基于雪崩三极管Marx脉冲发生器和脉冲陡化技术设计皮秒高压脉冲电路，通过优化电路参数，实现高幅值和窄半高宽的选通脉冲输出，并将该脉冲加载于MCP上，采用蒙特卡洛算法研究光电子动态倍增过程和计算MCP增益，以此获得MCP分幅相机时间分辨率。研究结果表明，基于雪崩三极管串并联结构的Marx脉冲发生器级数可决定脉冲输出幅值，脉冲陡化电路可对输出脉冲在时间上压缩，从而输出皮秒选通脉冲。当采用三级Marx脉冲发生器设计，脉冲陡化电路的两个电感，电容和负载分别为725 nH、7 nH、1 pF和200 Ω时，可获得幅值为－2.8 kV和半高宽为124 ps的皮秒选通脉冲。将选通脉冲加载于MCP，通过对不同时刻的光电子在MCP通道内动态倍增过程的分析和增益计算，获得MCP增益-时间归一化曲线的半高宽约为53 ps，即MCP分幅相机的时间分辨率。此外，由于选通脉冲的波形是V形，因此脉冲上升沿可应用于脉冲展宽分幅相机的展宽斜率，为进一步提升脉冲展宽分幅相机的时间分辨率提供条件。在今后的研究中，将针对如何提升系统对皮秒级高压脉冲的快速响应能力，以及如何降低寄生电感产生的可能性等实验难点，研制具有高幅值和窄半高宽的选通脉冲发生器。

参考文献

[1] WANG Feng, ZHANG Xing, LI Yulong, et al. Research progress of high space-time diagnostic technology in laser inertial confinement fusion research[J]. High Power Laser and Particle Beams, 2020, 32(11): 112002.
王峰, 张兴, 理玉龙, 等. 激光惯性约束聚变研究中高时空诊断技术研究进展[J]. 强激光与粒子束, 2020, 32(11): 112002.

[2] ZYLSTRA A B, HURRICANE O A, CALLAHAN D A, et al. Burning plasma achieved in inertial fusion[J]. Nature, 2022, 601:542-548.

[3] TIAN Jinshou. An overview of the development of streak and framing camera technology[J]. High Power Laser and Particle Beams, 2020, 32(11):32-48.
田进寿. 条纹及分幅相机技术发展概述[J]. 强激光与粒子束, 2020, 32(11):32-48.

[4] BENEDETTI L R, HOLDER J P, PERKINS M, et al. Advances in x-ray framing cameras at the National Ignition Facility to improve quantitative precision in x-ray imaging[J]. Review of Scientific Instruments, 2016, 87(2):023511.

[5] BELL P M, KILLKENNY J D. Measurements with a 35 psec gate time microchannel plate camera[C]. SPIE, 1990, 456: 1346.

[6] LIU Jinyuan, NIU Lihong, PENG Wenda, et al. Applicationof a fast electrical pulse in gated multichannel plate camera[J]. Review of Scientific Instruments, 2007, 78(5):055104.

[7] BUTKUS P, MURAUSKAS A, TOLVAISIENE S, et al. Concepts and capabilities of in-house built nanosecond pulsed electric field (nsPEF) generators for electroporation: state of art[J]. Applied Sciences, 2020, 10(12):4244.
[8] RAO Junfeng, ZHANg Wei, LI Zi, et al. Nanosecond pulse generator with series avalanche transistors[J]. High Power Laser and Particle Beams, 2018, 30(9):095002.
饶俊峰, 章薇, 李孜, 等. 雪崩三极管串联的纳秒脉冲发生器[J]. 强激光与粒子束, 2018, 30(9):095002.
[9] BEEV N, KELLER J, MEHLSTÄUBLER T E. Note: An avalanche transistor-based nanosecond pulse generator with 25 MHz repetition rate[J]. Review of Scientific Instruments, 2017, 88(12):126105.
[10] LI J T, ZHONG X, CAO H, et al. Development of a stereo-symmetrical nanosecond pulsed power generator composed of modularized avalanche transistor marx circuits[J]. Review of Scientific Instruments, 2015, 86(9):093502.
[11] MI Yan, BIAN Changhao, WAN Jialun, et al. Modular all-solid-state nanosecond pulse generator based on Blumlein and TLT[J]. Chinese Journal of Scientific Instrument, 2017, 38(11): 2858-2865.
米彦, 卞昌浩, 万佳仑, 等. 基于Blumlein和TLT的模块化全固态纳秒脉冲发生器[J]. 仪器仪表学报, 2017, 38(11): 2858-2865.
[12] ZOU L, GUPTA S, CALOZ C. A simple picosecond pulse generator based on a pair of step recovery diodes[J]. IEEE Microwave & Wireless Components Letters, 2017, 27(5):467-469.
[13] BOKHAN P A, GUGIN P P, ZAKREVSKY D E, et al. Generation of high-voltage pulses with a picosecond front in a cascade kivotron connection[J]. Instruments & Experimental Techniques, 2018, 61(4):491-495.
[14] YANG Wenzheng, HOU Xun, BAI Yonglin, et al. Uniform design of exposure time for microchannel plate gated X-ray picosecond framing cameras [J]. Acta Photonic Sinica, 2008,37(3):439-443.
杨文正, 侯洵, 白永林, 等. 微通道板选通X射线皮秒分幅相机曝光时间的均匀设计[J]. 光子学报, 2008,37(3):439-443.
[15] CAI H Z, FU W Y, WANG D, et al. Three-strip microchannel plate gated X-ray framing camera[J]. Sensors and Actuators A: Physical, 2019, 285:355-361.

Research on the Picoseconds Gating Pulse of Framing Camera Using Pulse Steepening Technique

CUI Fengxiang, BAI Yanli, WU Siqi, CHEN Huan, LIANG Luye, ZHU Yunfei, XIE Jun
(*School of Electronic Engineering and Automation, Guilin University of Electronic Technology, Guilin* 541004, *China*)

Abstract: Inertial confinement fusion is the main way to obtain experimental data of thermonuclear weapons. Since the Microchannel Plate (MCP) framing camera has picosecond-level temporal resolution and micron-level spatial resolution in the inertial confinement fusion experiment, it can effectively detect the plasma space-time evolution state of the Inertial confinement fusion process. The temporal resolution of the MCP framing camera is about 60~100 ps. The main influencing factors are the electronic transit time and its dispersion in the MCP channel. There are two main improvement methods: the thin MCP and optimized gating pulse. Although thin MCP can effectively improve the temporal resolution of the camera, it is difficult to be widely used due to the poor signal-to-noise ratio and high manufacturing process requirements. Therefore, the improvement of the temporal resolution of MCP framing cameras is commonly achieved by optimizing the circuit structure to obtain high-amplitude and narrow half-width picosecond gating pulse. High-voltage gating pulse with picoseconds is a branch of pulse power technology. Firstly, it usually stores low-power energy, and then releases energy to output high-power pulses in a very short time. The picosecond gating pulse applied to MCP framing camera can be realized by nanosecond high voltage pulse and pulse shaping. In terms of nanosecond high-voltage pulse, avalanche triodes are widely used in pulse generators due to their fast turn-on switching characteristics in avalanche states. However, under different circuit structures, high-voltage discharge ignition and easy breakdown can occur. In terms of pulse shaping, the output of picosecond pulse is usually realized through special line forming and pulse steepening technique. The former achieves a substantial reduction in pulse time width and power by compressing the pulse energy, while the latter achieves pulse time width compression by steepening the front and rear edges of the pulse, which has a relatively little impact on pulse power. The temporal resolution of the framing camera refers to the gain-time curve half width of the MCP. In order to calculate

the temporal resolution, a gating pulse is usually loaded on the MCP to study the photoelectron dynamic multiplication process in the MCP channel to calculate the electron gain, so as to draw the MCP gain-time curve. In this paper, Marx pulse generator is designed based on avalanche triode firstly, and the influence of circuit parameters on the output nanosecond pulse is analyzed. Marx generator is a common device used to obtain high amplitude and nanosecond half width pulses in pulse power technology. The n-stage Marx pulse generator is designed in a mixed mode of avalanche triode series and parallel connection. The avalanche breakdown voltage of the avalanche triode 2N5551 is about 480 V, which is used as a switch for the generator. In order to achieve a high amplitude output of the pulse generator and reduce the circuit complexity, it is required that each stage of the generating circuit should be connected in series with multiple avalanche triodes as much as possible to improve the output amplitude. However, due to the situation that too many avalanche triodes in series can lead to high-voltage ignition and reduce the stability of the generator, the number of avalanche triodes at all levels should not be too large. Considering comprehensively that 8 avalanche triodes are used in series to form a primary generator circuit in the design. When the generator stage n is 3, the output amplitude is about −6 kV, which has reached the output target. Considering that the output amplitude efficiency of the generator should be as large as possible and the half height width of the pulse should be as small as possible, a three-stage Marx pulse generator based on avalanche triode is used to realize nanosecond high-voltage pulse. The corresponding output pulse amplitude is −6.058 kV and full width at half maximum is 165.924 ns. A pulse shaping circuit is then designed based on the pulse steepening technology. The principle of pulse steepening is to rapidly charge and discharge small capacity capacitors through nanosecond pulses, shorten the pulse front time while losing part of the pulse amplitude, and shorten the pulse back time by reducing the trailing edge of the pulse. After steepening, the output pulse reaches picosecond. By analyzing the influence of circuit parameters on the picosecond gating pulse, the picosecond high-voltage gating pulse applied to the temporal resolution calculation of the microchannel plate framing camera is output, with an amplitude of −2.8 kV and a full width at half maximum of 124 ps. Monte Carlo method is used to establish the photoelectrons dynamic multiplication model in the MCP channel and the gating pulse is applied to the MCP gain calculation to obtain the temporal resolution. The process of obtaining the temporal resolution of the camera: first, the photoelectrons enter the MCP channel under the action of the gating pulse, and the photoelectrons collide with the MCP channel wall to generate secondary electrons; until the photoelectrons leave the MCP channel; finally, the MCP gain under the gating pulse at different times is calculated to obtain the temporal resolution of the MCP framing camera. The research results show that, the method of generating picosecond high voltage gating pulse by combining the Marx and the sharpening circuit is feasible. The gating pulse with an amplitude of −2.8 kV and a half-width of 124 ps is obtained when the Marx pulse generator is three stages, and the inductances and capacitance of the pulse sharpening circuit are 725 nH, 7 nH, and 1 pF respectively. The MCP gain time normalization curve with a half height width of about 53 ps is obtained by analyzing the dynamic multiplication process of photoelectrons in MCP channel at different times and calculating the gain, which is the temporal resolution of the MCP frame divider. In addition, since the waveform of the gating pulse is V-shaped, the pulse rising edge can be applied to the dilation gradient of pulse-dilation framing camera, which provides conditions for further improving the temporal resolution of pulse-dilation framing camera.

Key words: Framing camera; Pulse steepening technique; Gating pulse; The method of Monte Carlo; Temporal resolution

OCIS Codes: 250.0040; 040.1490; 320.7160; 260.7120

Foundation item: National Natural Science Foundation of China (No. 11865007), Natural Science Foundation of Guangxi Province (No. 2022GXNSFAA035561), Foundation of Guangxi Key Laboratory of Automatic Detecting Technology and Instruments (No. YQ22101)